flection coefficient as a function of frequency (Fig. 3) shows that there is an absorption peak ($S_{11} = -26$ dB) at 502 MHz, which is very close to the theoretical value $f = f_{T0} = 500$ MHz.

The dielectric constant was measured by an impedance-analyzing method in order to demonstrate the polariton excitation in ITPC. The results (Fig. 4) are compared with the theoretical results by choosing the proper damping term ($\gamma = 0.01\omega_{T0}$). The dielectric constant changed near ω_{T0}, caused by the superlattice in ITPC. The dielectric spectrum in this band has the same curve shape as the far-infrared dielectric constant of an ionic crystal caused by lattice vibration, showing that they have a similar origin. Much information on the ITPC can be obtained from the dielectric constant curve. The measured f_{T0}, f_{L0}, $\varepsilon(0)$, and $\varepsilon(\infty)$ values are 502 MHz, 547 MHz, 99.88, and 88.02, respectively. They all agree well to the theoretical predictions. The LST relation was also proved, which is $\omega_{L0}/\omega_{T0} = 1.09$, only a slight deviation from the value of $[\varepsilon(0)/\varepsilon(\infty)]^{1/2}$ (1.07). The absorption peak in Fig. 3 is at the same position of the peak of the $\varepsilon''(\omega)$, just as predicted. There is a gap between ω_{T0} and ω_{L0} where $\varepsilon < 0$ and incident EM waves will be strongly reflected. The phenomena above show that there is a polariton mode in ITPC.

From the similarity between the real ionic crystal and the ITPC, other long-wavelength optical properties (such as Raman and Brillouin scattering) might also be expected in an ITPC. The only difference is that they occur in different frequencies. For example, Raman scattering appears in the terahertz region for a real ionic crystal, whereas it might appear in the gigahertz region for an ITPC. Study on these effects is of fundamental interest in physics.

References and Notes

1. E. Yablonovitch, *Phys. Rev. Lett.* **58**, 2059 (1987).
2. _____, T. J. Gmitter, K. M. Leung, *ibid.* **67**, 2295 (1991); A. Mekis *et al.*, *ibid.* **77**, 3787 (1996); Y. S. Chan *et al.*, *ibid.* **80**, 956 (1998); M. M. Sigalas *et al.*, *Microwave Opt. Technol. Lett.* **15**, 153 (1997); J. S. Foresi *et al.*, *Nature* **390**, 143 (1997). For a review, see J. J. Joannopoulos *et al.*, *Photonic Crystals* (Princeton Univ. Press, Princeton, NJ, 1995).
3. M. M. Fejer *et al.*, *IEEE J. Quantum Electron.* **QE-28**, 2631 (1992).
4. D. Feng *et al.*, *Appl. Phys. Lett.* **37**, 607 (1980); Y. L. Lu *et al.*, *ibid.* **59**, 516 (1991); Y. L. Lu *et al.*, *ibid.* **68**, 1467 (1996); Y. Q. Lu *et al.*, *ibid.* **69**, 3155 (1996); Y. Lu *et al.*, *Science* **276**, 2004 (1997).
5. L. Ye *et al.*, *Phys. Rev. Lett.* **69**, 3080 (1992).
6. M. S. Kushwaha *et al.*, *ibid.* **71**, 2022 (1993).
7. M. M. Sigalas *et al.*, *Phys. Rev. B* **50**, 3393 (1994); M. S. Kushwaha and P. Halevi, *Appl. Phys. Lett.* **64**, 1085 (1994); J. P. Dowling, *J. Acoust. Soc. Am.* **91**, 2539 (1992); M. M. Sigalas, *ibid.* **101**, 1256 (1997); F. R. Montero de Espinosa *et al.*, *Phys. Rev. Lett.* **80**, 1208 (1998).
8. P. Sheng, Ed., *Scattering and Localization of Classical Waves in Random Media* (World Scientific, Singapore, 1990).
9. S. N. Zhu *et al.*, *Science* **278**, 843 (1997); S. N. Zhu *et al.*, *Phys. Rev. Lett.* **78**, 2752 (1997).
10. K. M. Ho *et al.*, *Phys. Rev. Lett.* **65**, 3152 (1990).
11. J. B. Pendry and A. Mackinnon, *ibid.* **69**, 2772 (1992); H. Dong and S. Xiong, *J. Phys. Condens. Matter* **5**, 8849 (1993); M. M. Sigalas and C. M. Soukoulis, *Phys. Rev. B* **51**, 2780 (1995).
12. J. D. Turner and A. J. Pretlove, *Acoustics for Engineers* (Macmillan, Houndmills, UK, 1991), pp. 27–29; L. Meirovitch, *Elements of Vibration Analysis* (McGraw-Hill, New York, 1975), pp. 281–284.
13. K. Huang, *Proc. R. Soc. London A* **208**, 352 (1951); M. Born and K. Huang, *Dynamical Theory of Crystal Lattices* (Oxford Univ. Press, Oxford, 1954).
14. C. H. Henry and J. J. Hopfield, *Phys. Rev. Lett.* **15**, 964 (1965).
15. $\varepsilon = 84.1$, $\varepsilon_0 = 8.854 \times 10^{-12}$ F/m, $v = 3600$ m/s, $e_{15} = 3.8$ C/m², $\rho = 4.64 \times 10^3$ kg/m³ [Y. Nakagawa *et al.*, *J. Appl. Phys.* **44**, 3969 (1973)].
16. We are grateful to the State Key Program for Basic Research of China, the National Natural Science Foundation Project of China (contract 69708007), and the National Advanced Materials Committee of China for their support of this work.

1 February 1999; accepted 27 April 1999

Middle Eocene Seawater pH and Atmospheric Carbon Dioxide Concentrations

Paul N. Pearson[1]* and Martin R. Palmer[2]

The carbon dioxide content of the atmosphere [measured as the partial pressure of CO_2 (pCO_2)] affects the content of the surface ocean, which in turn affects seawater pH. The boron isotope composition ($\delta^{11}B$) of contemporaneous planktonic foraminifera that calcified their tests at different water depths can be used to reconstruct the pH-depth profile of ancient seawater. Construction of a pH profile for the middle Eocene tropical Pacific Ocean shows that atmospheric pCO_2 was probably similar to modern concentrations or slightly higher.

Earth's climate has cooled markedly in the last 50 million years from a peak of warmth in the early Eocene (*1*). One explanation for this cooling invokes plate tectonic movements and reorganization of ocean currents (*2*). Another is that concentrations of greenhouse gases, especially CO_2, have declined in the atmosphere (*3–5*).

The period of greatest uncertainty in CO_2 concentrations is the middle to late Eocene, which followed an interval of extreme warmth in the early Eocene but preceded dramatic cooling in the earliest Oligocene (*6*). There is much less evidence for widespread hydrothermal, tectonic, and volcanic activity (and hence CO_2 emission) in this interval than in the Cretaceous to early Eocene (*7–10*), and yet world climate was still warm and equable compared with that of the present day (*11*). Some authors have suggested that middle Eocene pCO_2 was two to six times as high as the preindustrial level of 280 ppm (*3, 12–16*), whereas others have suggested values similar to that concentration or only slightly higher (*17–19*). These estimates rely on a variety of relatively indirect methods such as carbon mass balance modeling (*3, 13, 15, 18–19*), interpretation of the $\delta^{13}C$ record in marine sediments (*12, 14*) and paleosols (*17*), or studies of plant leaf morphology (*16*).

The $\delta^{11}B$ of foraminiferal calcite may provide a more direct measure of atmospheric pCO_2 because it reflects the pH of the surface seawater in which the organisms calcified, which is closely dependent on pCO_2 (*20*). By analyzing multiple species that lived at different depths in the ocean, it is possible to reconstruct a pH-depth profile for the upper few hundred meters of the water column (*21*). This allows paleo sea surface pH to be estimated with some confidence, from which pCO_2 can be inferred.

We selected a sample of well-preserved pelagic carbonate from the middle Eocene of the tropical Pacific [Ocean Drilling Program sample 143-865C-6H/2, 65 to 67 cm; lower Biozone P12; dated to approximately 43 million years ago (Ma)]. The sample has a diverse foraminiferal assemblage, which indicates a warm, oligotrophic and well-stratified water column, an inference that is supported by sedimentological and geochemical evidence (*22*). Monospecific splits of 50 to 250 specimens of a variety of species were picked for $\delta^{11}B$ analysis (*21*) (Table 1). Plankton species were assigned to calcification depths (mixed layer, intermediate, thermocline, and deep) on the basis of previous paleobiological research and $\delta^{18}O$ and $\delta^{13}C$ analyses (*22–27*). A single split of benthic foraminifera was also prepared, but because they are scarce in the

[1]Department of Earth Sciences, University of Bristol, Bristol BS8 1RJ, UK. [2]T. H. Huxley School, Royal School of Mines, Imperial College, Prince Consort Road, London SW7 2BP, UK.

*To whom correspondence should be addressed. E-mail: paul.pearson@bristol.ac.uk

sample, the split consists of mixed species.

The principal control on the $\delta^{11}B$ of foraminiferal calcite is pH (20), but temperature, pressure, and salinity also influence the value (in order of decreasing importance) because of their effects on the pK_a (K_a is the dissociation constant) of boric acid (28) and boron isotope fractionation (29). Therefore, to estimate pH it is necessary to assign absolute depths and temperatures for the various plankton habitats. We did this by assuming that the temperature and salinity of the Eocene upper water column were similar to that of the modern western tropical Pacific, but that bottom waters were warmer, at 11°C (11). The exact choice of temperature and salinity profiles makes little difference to our final estimate of surface pH.

Initially it can be assumed that the $\delta^{11}B$ of seawater ($\delta^{11}B_{sw}$) in the middle Eocene was the same as that of modern oceans (39.5 per mil). The data (Fig. 1) show a clear decline in pH from the surface to subthermocline depths and thus support the relative depth ranking of Eocene planktonic foraminifera that has previously been established from $\delta^{18}O$ and $\delta^{13}C$ analyses (22–27). The internal consistency of

the data set also argues against significant diagenetic alteration of the $\delta^{11}B$ values. The only species with anomalous $\delta^{11}B$ is *Morozovella crassata*, which we classify as a mixed-layer dweller like other related species in the genera *Acarinina* and *Morozovella*, but it has a more negative $\delta^{11}B$ value than these species and the four intermediate dwelling species. At present we cannot account for the divergent $\delta^{11}B$ of *M. crassata*, but one possibility is that it was subject to an unknown vital effect in fractionating boron isotopes.

A critical variable in the calculation of paleo-pH values is the $\delta^{11}B_{sw}$ value. Boron has a long residence time in the ocean (~20 Ma); hence, rapid fluctuations in $\delta^{11}B_{sw}$ are not expected. However, a gradual drift in $\delta^{11}B_{sw}$ values may have occurred since the Eocene. To investigate this, we calculated alternative pH profiles based on $\delta^{11}B_{sw}$ of 41.0, 39.5, and 38.0 per mil (Fig. 2). From these profiles, we deduce that a $\delta^{11}B_{sw}$ value less than 38.0 per mil is unlikely because it would imply an anomalously shallow pH gradient and low levels of biological productivity. Similarly, it is unlikely that $\delta^{11}B_{sw}$ was greater than 41.0 per mil because this would imply acidic conditions (pH < 7) in the oxygen minimum zone, which would have inhibited foraminiferal calcification. If we assume that the difference in pH between the mixed layer and the depth of minimum pH is due predominantly to the oxidation of organic matter (30), the apparent oxygen utilization (AOU) can be calculated (31). With this approach a $\delta^{11}B_{sw}$ of 41.0 per mil would imply an AOU of 240 μM per kilogram of organic matter. This is close to the maximum AOU

(250 μM/kg) observed at this depth in the equatorial Pacific high-productivity zone and well above the average AOU for better stratified parts of the ocean (31). These observations provide further support for the hypothesis that $\delta^{11}B_{sw}$ in the middle Eocene was not greater than 41.0 per mil.

Our minimum estimate for surface seawater pH (pH$_{min}$) in the middle Eocene is given by assuming a $\delta^{11}B_{sw}$ of 41.0 per mil and calculating the mean of all four mixed-layer values (including *M. crassata*), thus pH$_{min}$ = 7.91. For the maximum estimate (pH$_{max}$) we assume that $\delta^{11}B_{sw}$ = 38.0 per mil, disregard the *M. crassata* value as a probable vital effect, and average the remaining three mixed-layer dwellers, thus pH$_{max}$ = 8.33. In our best estimate (pH$_{best}$) for surface water pH, we assume that AOU = 100 μM/kg at the pH minimum [consistent with the evidence for an oligotrophic water column at the

Fig. 3. Calculation of the variation of surface seawater pCO$_2$ with ΣCO$_2$ based on various estimates of sea surface pH.
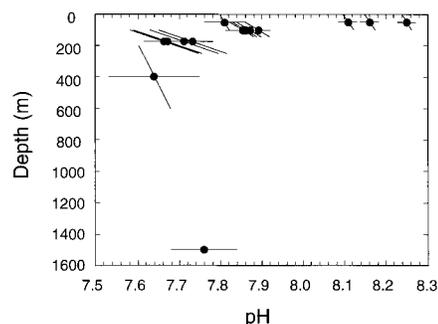

Fig. 1. Calculated pH profile for the middle Eocene of sample 143-865C-6H/2, 65 to 67 cm, based on $\delta^{11}B$ data in Table 1. See (21) for details of the calculation procedure. For the profile, a value of $\delta^{11}B_{sw}$ of +39.5 per mil was assumed.
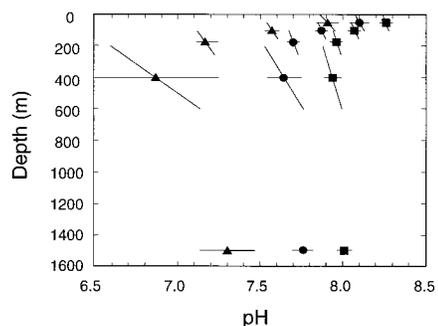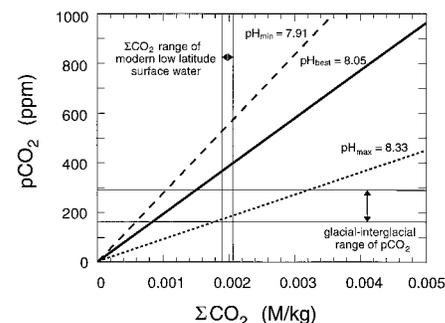

Fig. 2. Effect of varying $\delta^{11}B_{sw}$ on the estimated pH profile. Each value is calculated from the mean $\delta^{11}B$ of the species in each depth class. Triangles: $\delta^{11}B_{sw}$ = 41.0 per mil; circles: $\delta^{11}B_{sw}$ = 39.5 per mil; squares: $\delta^{11}B_{sw}$ = 38.0 per mil.

Table 1. Depth classes and boron isotope data for different species picked from sample 143-865C-6H/2, 65 to 67 cm.

Species	Size fraction (μm)	$\delta^{11}B$ (±2σ)	Mean $\delta^{11}B$
Mixed layer (0 to 100 m)			
Morozovella spinulosa	300–425	26.6 ± 0.4, 26.2 ± 0.3	26.4
Acarinina matthewsae	355–500	25.8 ± 0.4, 25.4 ± 0.4	25.6
Acarinina topilensis	355–550	25.3 ± 0.3, 24.9 ± 0.4	25.1
Morozovella crassata	300–500	23.2 ± 0.4, 22.6 ± 0.4	22.9
Intermediate (50 to 150 m)			
Globigerinatheka index	425–500	23.4 ± 0.4, 23.1 ± 0.4	23.3
Globigerinatheka mexicana	425–500	23.3 ± 0.4, 23.0 ± 0.4	23.2
Globigerinatheka senni	300–355	23.4 ± 0.4, 22.8 ± 0.4	23.1
Turborotalia pomeroli	300–500	23.3 ± 0.4, 22.9 ± 0.4	23.1
Thermocline (100 to 250 m)			
Dentoglobigerina galavisi	300–500	21.9 ± 0.6, 22.0 ± 0.4	22.0
Hantkenina dumblei	250–600	21.9 ± 0.6, 21.9 ± 0.3	21.9
Subbotina patagonica	300–425	21.4 ± 0.4, 22.0 ± 0.8	21.7
Subbotina bakeri	300–355	21.7 ± 0.4, 21.7 ± 0.3	21.7
Deep (200 to 600 m)			
Catapsydrax unicavus	355–500	20.8 ± 0.4, 21.7 ± 0.4	21.3
Sea floor			
Mixed species	250–600	21.2 ± 0.6, 22.0 ± 0.8	21.6

site (*24*)]. Thus, $\delta^{11}B_{sw}$ is estimated at 40.6 per mil, and disregarding the $\delta^{11}B$ value for *M. crassata*, $pH_{best} = 8.05$.

Two of four key chemical variables [pCO_2, pH, the total alkalinity ($\Sigma_{alkalinity}$), and the total dissolved inorganic carbon (ΣCO_2)] are required to define the thermodynamics of the CO_2 system in the ocean (*31*). As we only have an estimate of paleo-pH from our Eocene sample, pCO_2 can only be calculated as a function of one of the other two key variables (*32*) (Fig. 3). Assuming that ΣCO_2 values were the same as the modern ocean, for pH_{min} of 7.91 we calculate pCO_2 as 530 to 570 ppm. To achieve a value of five times modern pCO_2 we would have to invoke ΣCO_2 concentrations of more than twice the modern value, which is unreasonable because it would imply a larger variation in calcium carbonate saturation in the oceans than is compatible with the geologic record (*33*). Assuming pH_{max} for our sample of 8.33 and modern ΣCO_2 concentrations, we obtain a minimum estimate of pCO_2 of 170 to 190 ppm. Our pH_{best} estimate of 8.05 with modern ΣCO_2 gives a pCO_2 of 370 to 400 ppm, only slightly higher than modern concentrations.

Seasonal temperature cycles and biological processes mean that the pCO_2 of seawater in the surface mixed layer is not in perfect equilibrium with the atmosphere, but this deviation is generally <10% in the absence of upwelling of CO_2-rich deep waters (*31*). As our sample splits were not taken from an upwelling area and represent the average pH recorded by many individuals that lived at different times, the calculated pCO_2 values give reasonable estimates of the mid-Eocene atmosphere, provided ΣCO_2 was not greatly different from the modern value. If our estimate of middle Eocene pCO_2 is correct, then it implies either that Earth's climate is very sensitive to small changes in pCO_2, or that the global cooling since the Eocene was not driven primarily by changes in pCO_2, but rather reflects reorganization of ocean circulation resulting from tectonic opening and closing of oceanic gateways (*2*).

References and Notes

1. K. G. Miller, R. G. Fairbanks, G. S. Mountain, *Paleoceanography* **2**, 1 (1987).
2. J. P. Kennett, *Marine Geology* (Prentice-Hall, Englewood, NJ, 1982), p. 695.
3. R. A. Berner, A. C. Lasaga, R. M. Garrels, *Am. J. Sci.* **283**, 641 (1983).
4. E. J. Barron, *Palaeogeogr. Palaeoclimatol. Palaeoecol.* **50**, 45 (1985).
5. M. E. Raymo and W. F. Ruddiman, *Nature* **359**, 117 (1992).
6. W. A. Berggren and D. R. Prothero, in *Eocene-Oligocene Climatic and Biotic Evolution*, D. R. Prothero and W. A. Berggren, Eds. (Princeton Univ. Press, Princeton, NJ, 1992), p. 1.
7. R. M. Owen and D. H. Rea, *Science* **227**, 166 (1985).
8. D. K. Rea *et al.*, *Palaeogeogr. Palaeoclimatol. Palaeoecol.* **79**, 117 (1990).
9. O. Eldholm and E. Thomas, *Earth Planet. Sci. Lett.* **117**, 319 (1993).
10. D. M. Kerrick and K. Caldeira, *Chem. Geol.* **145**, 213 (1998).
11. J. C. Zachos *et al.*, *J. Geol.* **101**, 191 (1993).
12. M. A. Arthur *et al.*, *Eos* **72**, 166 (1991).
13. P. V. Brady, *J. Geophys. Res.* **96**, 18101 (1991).
14. K. H. Freeman and J. M. Hayes, *Global Biogeochem. Cycles* **6**, 185 (1992).
15. T. R. Worsley *et al.*, *Geol. Soc. Am. Spec. Pap.* **288**, 57 (1994).
16. J. C. McElwain, *Philos. Trans. R. Soc. London Ser. B* **353**, 83 (1998).
17. R. A. Berner, *Am. J. Sci.* **291**, 339 (1991).
18. T. E. Cerling, *ibid.* **293**, 377 (1993).
19. R. A. Berner, *ibid.* **294**, 56 (1994).
20. Boron exists as two main species in seawater, $B(OH)_3$ and $B(OH)_4^-$, the relative abundance of which is controlled primarily by pH [J. F. Hershey, M. Fernandez, P. J. Milne, F. J. Millero, *Geochim. Cosmochim. Acta* **50**, 143 (1986)]. There is a strong isotopic fractionation between the two species, in which ^{10}B prefers tetrahedral coordination by about -19.8 per mil relative to ^{11}B (*29*). On the basis of analysis of a variety of modern marine carbonates, N. G. Hemming and G. N. Hansen [*ibid.* **56**, 537 (1992)] suggested that boron incorporation into carbonate is from $B(OH)_4^-$ and consequently that the $\delta^{11}B$ of calcite is a pH indicator. A. J. Spivack, C. F. You, and H. J. Smith [*Nature* **363**, 149 (1993)] suggested that boron isotope measurements of seawater pH could be used to infer past pCO_2. The pH relation was tested by A. Sanyal *et al.* [*Paleoceanography* **11**, 513 (1996)] using the living planktonic foraminifer *Orbulina universa*, batches of which were cultured from the juvenile stage to maturity over a controlled range of pH conditions. This experiment confirmed the predicted relation between the $\delta^{11}B$ of shell calcite and pH, except that a consistent offset from the expected $\delta^{11}B$ value of -4 per mil was observed. Sanyal and others interpreted this offset as a probable vital effect. It may have been caused by dissolution of previously formed calcite in *O. universa* as it constructs its final chamber. Further work by A. Sanyal, N. G. Hemming, W. S. Broecker, and G. N. Hanson [*Global Biogeochem. Cycles* **11**, 125 (1997)] suggests that the offset is peculiar to *O. universa* and that other species construct their shells at or close to equilibrium $\delta^{11}B$ of $B(OH)_4^-$. The value of $\delta^{11}B$ is calculated as follows:

$$\delta^{11}B = \left[\frac{(^{11}B/^{10}B)_{sample}}{(^{11}B/^{10}B)_{standard}} - 1 \right] \times 1000$$

where $(^{11}B/^{10}B)_{standard} = 3.9873$ for the standard NBS SRM 951.
21. M. R. Palmer, P. N. Pearson, S. J. Cobb, *Science* **282**, 1468 (1998).
22. T. J. Bralower *et al.*, *Paleoceanography* **10**, 841 (1995).
23. A. Boersma, I. Premoli Silva, N. J. Shackleton, *ibid.* **2**, 287 (1987).
24. P. N. Pearson, N. J. Shackleton, M. A. Hall, *J. Foraminifer. Res* **23**, 123 (1993).
25. A. J. M. van Eijden, *Palaeogeogr. Palaeoclimatol. Palaeoecol.* **113**, 267 (1995).
26. G. Lu and G. Keller, *J. Foraminiferal. Res.* **26**, 103 (1996).
27. P. N. Pearson, *Paleontol. Soc. Pap.* **4**, 138 (1998).
28. F. J. Millero, *Geochim. Cosmochim. Acta* **59**, 661 (1995).
29. H. Kakihana *et al.*, *Bull. Chem. Soc. Jpn.* **50**, 158 (1977).
30. P. M. Kroopnick, *Deep Sea Re.* **32**, 57 (1985).
31. W. S. Broecker and T. H. Peng, *Tracers in the Sea* (Columbia Univ. Press, New York, 1982).
32. The partial pressure of carbon dioxide and the concentration of total dissolved inorganic carbon are related by the equation

$$pCO_2 = K_H \left(1 + \frac{K_1}{[H^+]} + \frac{K_1 K_2}{[H^+]^2} \right)^{-1} \Sigma CO_2$$

where K_H is the Henry's law constant for CO_2, and K_1 and K_2 are the first and second dissociation constants for carbonic acid.
33. T. J. van Andel, *Earth Planet. Sci. Lett.* **26**, 187 (1975).
34. Supported by a grant from the Natural Environment Research Council. The sample used in this research was supplied by the Ocean Drilling Program. We are grateful to S. Cobb for help in sample preparation and to two anonymous reviewers.

Regular and Irregular Patterns in Semiarid Vegetation

Christopher A. Klausmeier

Vegetation in many semiarid regions is strikingly patterned, forming regular stripes on hillsides and irregular mosaics on flat ground. A simple model of plant and water dynamics based on ecologically realistic assumptions and with reasonable parameter values captures both of these types of patterns. The regular patterns result from a Turing-like instability; the irregular patterns arise when the ecological dynamics amplify slight small-scale topographic variability. Because of the close agreement between observations and these theoretical results, this system provides a clear example of how nonlinear mechanisms can be important in determining the spatial structure of plant communities.

Pattern formation has long interested both theoretical biologists (*1*, *2*) and plant ecologists (*3*, *4*). Theoretical studies have shown that local interactions coupled by dispersal can cause nonuniform distributions of organisms to develop in the absence of underlying heterogeneity. Recently it has been shown that such an interaction between a herbivorous insect and its parasitoid localizes outbreaks of the herbivore, in accordance with mathematical models (*5*). However, in general, close agreement between the mathematical theory and observation or experiment has been rare (*6*). Furthermore, most of these studies have focused on interactions between animal populations, not on the interaction of plants and their abiotic resources.

Vegetation patterns are found in many semiarid regions including parts of Africa (*7*–

Department of Ecology, Evolution and Behavior, University of Minnesota, St. Paul, MN 55108, USA. E-mail: klaus@biosci.umn.edu